Analysis of Temperature-Dependent Thermal Post-Buckling and Flutter Boundary of FG panel under Supersonic Airflows

Sang-Lae Lee and Ji-Hwan Kim

School of Mechanical and Aerospace Engineering, Seoul National University,

San 56-1, Shinlim-dong, Kwanak-ku, Seoul 151-742, South Korea

Abstract

In this study, it is investigated the thermal post-buckling characteristics and flutter boundary of Functionally Graded (FG) panel under the heats and supersonic airflows. Material properties are assumed to be temperature dependent, and a simple power law distribution is taken as in the previous research works. First-order shear deformation theory (FSDT) of plate is applied to model the panel, and the von-Karman strain-displacement relations are adopted to consider the geometric nonlinearity due to large deformation. Further, the first-order piston theory is used to model the supersonic aerodynamic load acting on a panel. In order to find a critical flutter speed, linear flutter analysis of FG panels is performed. Numerical results are compared with the previous works, and present results for the temperature dependent material are discussed in detail for thermal post-buckling behavior and flutter boundary of the panel with various volume fractions, and aerodynamic pressures.

1. Introduction

To overcome the drawbacks of the composite materials, Functionally Graded Materials (FGMs) have been developed (Miyamoto et al). Typically, an FGM is made up of ceramic and metal for the purpose of thermal protection against large temperature gradients. That is to say, the ceramic has a role to withstand significant heat conduction while the metal keeps a certain extent of toughness in a high-temperature environment. Mixture of the materials, so

called FGM, varies continuously from one interface to the other using gradual variation of the volume fraction for constituent materials. Application fields of FGMs are skin panels of spacecraft, supersonic and hypersonic flight vehicle, jet engine, nuclear plants and fusion reactors, etc. Therefore, the post-buckling and flutter boundary analyses of the FG panel with temperature dependent material properties under the supersonic aerodynamic loads will be one of the interesting topics.

Up to now, modeling, thermal buckling, thermal post-buckling, vibration and nonlinear vibration analyses of FGMs have been studied vigorously. Praveen and Reddy investigated the static and dynamic thermo-elastic response of plates considering geometrical nonlinearity for a large deflection. However, the change of material properties due to temperature distribution was not considered in the analysis. Feldman and Aboudi studied elastic bifurcation buckling of plates under in-plane compressive loading. Na and Kim tried to model the panel more accurately using 18 nodes three dimensional solid element in the finite element method, and the behavior of panel for the thermal buckling and post-buckling were investigated under a non-uniform temperature rise. Chen analyzed the nonlinear vibration of a shear deformable plate including rotary inertia effect. It was found that the volume fractions of constituents greatly change the behavior of nonlinear vibration. Wu Lanhe studied the thermal buckling of a simply supported plate under the two types of thermal loading such as uniform or gradient temperature rise through the thickness of the plate. Park and Kim investigated thermal post-buckling and vibration behaviors of the plate. Considering initial displacements and initial stresses, incremental form was adopted for the nonlinear temperature dependent material properties. Kim studied the temperature dependent vibration of plate based on a higher-order theory. Shen dealt with thermal post-buckling behavior of higher order shear deformable simply-supported plate with temperature dependent material properties including geometric imperfections.

Furthermore, supersonic flutter characteristics of FG panels were studied by Prakash and

Ganapathi using FEM. They considered linear strains and showed that the use of FGM increases the flutter margin in comparison with metals. Non-linear oscillations of a FG panel were investigated by Haddadpour et al. They showed that four to six mode shapes should be employed for quantitative accuracy to compute the aero-elastic response of the plate in the range of parameters studied. Also, at an instance of time when the FG panel reaches its maximum deflection during flutter, the stress of the top (bottom) surface is not the symmetric to that of the bottom (top) surface at the same time about a non-zero mean. Sohn and Kim dealt with the structural flutter of the panels for temperature independent material characteristics. The influence of the aerodynamic loads and effect of asymmetric properties of the materials on flutter characteristics of the panel are examined in detail. Especially, snap-through phenomena are reported to occur in the simply supported panel.

Generally, FGMs have been used in high temperature environments, and thus the material properties have to depend on the temperature. In this study, thermal post-buckling behaviors and flutter boundary of FG panels are examined under the influence of the aerodynamic loads. In addition, material characteristics were assumed to be continuously varying in the thickness direction of the panel according to a simple power law distribution in terms of the volume fraction of the constituent. Temperature dependent material properties are chosen for the description of the panel model. First-order shear deformation theory (FSDT) and the von-Karman strain-displacement relations are adopted to consider the geometric nonlinearity of the panel. To consider the supersonic aerodynamic load, the first-order piston theory is used. Numerical results are compared with the previous works, and present results for the temperature dependent material are discussed with the various volume fractions, and aerodynamic pressures.

2. Formulation

Fig.1 shows a coordinate system and geometry of a ceramic-metal FGM rectangular panel model with a length a, width b and thickness h subjected to supersonic airflow and thermal loads.

2.1. Material Properties of FG Plates

A simple power law distribution is adopted, the volume fractions of the ceramic and metal are expressed by Reddy :

$$V_c(z)=\left(\frac{z}{h}+\frac{1}{2}\right)^k \qquad (0\le k<\infty), \qquad V_c+V_m=1 \tag{1}$$

where, V, the superscript k, the subscripts c and m denote the volume fraction, the volume fraction index, ceramic and metal, respectively. Therefore, at the top surface ($z=h/2$) and the bottom surface ($z=-h/2$) are ceramic-rich and metal-rich, respectively. The material properties of FG plates can be obtained by a linear rule of mixture (Reddy) as follows:

$$P_{\text{eff}}(T,z)=P_m(T)V_m(z)+P_c(T)V_c(z)=P_c(T)+(P_m(T)-P_c(T))\left(1-\frac{z}{h}\right)^k \tag{2}$$

where, P_{eff}, P_m and P_c are the effective material property, the material properties of the metal and ceramic, respectively.

Material properties of constituents must be dependent on temperature as well as position for FGMs in high temperature environments. The properties, P, of the ceramics and metals used as a mixture of FGMs can be expressed as (Touloukian) ;

$$P(T)=P_0\left(\frac{P_{-1}}{T}+1+P_1T+P_2T^2+P_3T^3\right) \tag{3}$$

in which P_0, P_{-1}, P_1, P_2 and P_3 are the effective material properties and the coefficients of temperature.

Using the Eqs. (1)–(3), the modulus of elasticity E, the coefficient of thermal expansion

α , the density ρ and the thermal conductivity K are written as

$$
\begin{aligned}
E(T,z) &= (E_c(T) - E_m(T))\left(\frac{z}{h} + \frac{1}{2}\right)^k + E_m(T) \\
\alpha(T,z) &= (\alpha_c(T) - \alpha_m(T))\left(\frac{z}{h} + \frac{1}{2}\right)^k + \alpha_m(T) \\
\rho(T,z) &= (\rho_c(T) - \rho_m(T))\left(\frac{z}{h} + \frac{1}{2}\right)^k + \rho_m(T) \\
K(z) &= (K_c - K_m)\left(\frac{z}{h} + \frac{1}{2}\right)^k + K_m
\end{aligned}
\tag{4}
$$

Here the thermal conductivity K are assumed to be independent of temperature and the Posson's ratio ν is assumed to be constant as 0.3. Table. 1 shows data for different kinds of material properties used in this paper.

2.2. Constitutive Equations

Based on the first-order shear deformation theory of plate, the displacement fields for the panel can be expressed as:

$$
\begin{aligned}
u(x,y,z,t) &= u_0(x,y,t) + z\phi_x(x,y,t) \\
v(x,y,z,t) &= v_0(x,y,t) + z\phi_y(x,y,t) \\
w(x,y,z,t) &= w_0(x,y,t)
\end{aligned}
\tag{5}
$$

where u, v and w are the displacements in the x, y, and z directions and ϕ_x, ϕ_y are the rotations of the normal in the xz and yz planes, respectively, while the subscript '0' denotes the mid-plane.

Using the von Karman strain-displacement relations, the strain vectors are expressed as:

$$
\begin{aligned}
\{e\} &= \{\varepsilon\} + z\{\kappa\} \\
\{\gamma\} &= \{\gamma_{yz}, \gamma_{xz}\}^T
\end{aligned}
\tag{6.a}
$$

where, $\{\varepsilon\}$ and $\{\kappa\}$ are the in-plane strain, the curvature strain at the mid-plane, respectively. Additionally, $\{\varepsilon\}$, $\{\kappa\}$ and $\{\gamma\}$ are given as:

$$\{\varepsilon\} = \{u_{,x} + \frac{1}{2}w_{,x}{}^2 \ , \ v_{,y} + \frac{1}{2}w_{,y}{}^2 \ , \ u_{,y} + v_{,x} + w_{,y}w_{,x}\}^T$$
$$\{\kappa\} = \{\phi_{x,x} \ , \ \phi_{y,y} \ , \ \phi_{x,y} + \phi_{y,x}\}^T \tag{6.b}$$
$$\{\gamma\} = \{w_{,y} + \phi_y \ , \ w_{,x} + \phi_x\}^T$$

The constitutive equations for the FG plates can be written as,

$$\begin{Bmatrix} \mathbf{N} \\ \mathbf{M} \end{Bmatrix} = \begin{bmatrix} \mathbf{A} & \mathbf{B} \\ \mathbf{B} & \mathbf{D} \end{bmatrix} \begin{Bmatrix} \boldsymbol{\varepsilon} \\ \boldsymbol{\kappa} \end{Bmatrix} - \begin{Bmatrix} \mathbf{N}_{\Delta\mathbf{T}} \\ \mathbf{M}_{\Delta\mathbf{T}} \end{Bmatrix} \tag{7.a}$$

$$\mathbf{Q} = \mathbf{S}\boldsymbol{\gamma} \tag{7.b}$$

where, $\mathbf{N_b}$, $\mathbf{M_b}$ and $\mathbf{Q}$ denote the in-plane force resultant, the moment resultant and the transverse shear force resultant vectors, respectively. Meanwhile, $\mathbf{N}_{\Delta\mathbf{T}}$ and $\mathbf{M}_{\Delta\mathbf{T}}$ are the thermal in-plane force resultant and the thermal moment resultant vectors, which are given as:

$$(\mathbf{N}_{\Delta\mathbf{T}} \ , \ \mathbf{M}_{\Delta\mathbf{T}}) = \left\{N_{\Delta Tx}, N_{\Delta Ty}, N_{\Delta Txy}\right\}^T = \int_{-h/2}^{h/2} (1, z)\mathbf{E}\left\{\alpha(z), \alpha(z), 0\right\}^T \Delta T(z)\, dz \tag{8}$$

The temperature elevation is defined as $\Delta T(z) = T(z) - T_0$ where T_0 is the reference temperature and $T(z)$ is the temperature distribution through the thickness.

The elastic coefficient matrix is

$$\mathbf{E} = \frac{E(z)}{1-\nu^2}\begin{bmatrix} 1 & \nu & 0 \\ \nu & 1 & 0 \\ 0 & 0 & \dfrac{1-\nu}{2} \end{bmatrix}$$

while, $\mathbf{A}$, $\mathbf{B}$, $\mathbf{D}$ and $\mathbf{S}$ are the in-plane, the in-plane-bending coupling stiffness, the bending stiffness and the transverse shear stiffness matrices, which are given as:

$$(\ \mathbf{A},\ \mathbf{B},\ \mathbf{D}\ ) = \int_{-h/2}^{h/2} \mathbf{E}(\ 1,\ z,\ z^2)dz \tag{9}$$

$$\mathbf{S} = \kappa_p \int_{-h/2}^{h/2} \frac{E(z)}{2(1+\nu)}\begin{bmatrix} 1 & 0 \\ 0 & 1 \end{bmatrix} dz \tag{10}$$

where, $E(z)$ is the elastic modulus of an FG panel and the shear correction factor , κ_p, is

assumed as 5/6.

The temperature variation is assumed to occur in the thickness direction only and the temperature field is considered constant in the xy plane. In this case, the temperature through thickness is governed by the one-dimensional Fourier equation of heat conduction:

$$\frac{d}{dz}\left[K(z)\frac{dT}{dz}\right]=0\ ,\quad \begin{matrix} T=T_c \text{ at } z=h/2 \\ T=T_m \text{ at } z=-h/2 \end{matrix} \tag{11.a}$$

where, T_m and T_c are temperature of the metal and ceramic, respectively.

Using the solution in (Javaheri and Eslami), temperature distribution across the plate thickness becomes :

$$T(z)=T_m+(T_c-T_m)\Gamma(z) \tag{11.b}$$

where,

$$\Gamma(z)=\frac{1}{C}\left[\begin{matrix}\left(\frac{2z+h}{2h}\right)-\frac{K_{cm}}{(k+1)K_m}\left(\frac{2z+h}{2h}\right)^{k+1}+\frac{K_{cm}^2}{(2k+1)K_m}\left(\frac{2z+h}{2h}\right)^{2k+1} \\ -\frac{K_{cm}^3}{(3k+1)K_m}\left(\frac{2z+h}{2h}\right)^{3k+1}+\frac{K_{cm}^4}{(4k+1)K_m}\left(\frac{2z+h}{2h}\right)^{4k+1}-\frac{K_{cm}^5}{(5k+1)K_m}\left(\frac{2z+h}{2h}\right)^{5k+1}\end{matrix}\right]$$

$$C=1-\frac{K_{cm}}{(k+1)K_m}+\frac{K_{cm}^2}{(2k+1)K_m^2}-\frac{K_{cm}^3}{(3k+1)K_m^3}+\frac{K_{cm}^4}{(4k+1)K_m^4}-\frac{K_{cm}^5}{(5k+1)K_m^5}$$

for $K_{cm}=K_c-K_m$.

2.3. Governing Equations

Applying principle of virtual work for FG panel, the governing equations are obtained:

$$\delta W=\delta W_{\text{int}}-\delta W_{\text{ext}}=0 \tag{12}$$

where δW_{int} and δW_{ext} represent internal and external virtual work respectively, and are given as,

$$\begin{aligned}\delta W_{\text{int}} &= \int_V \delta\mathbf{e}^{\mathbf{T}}\boldsymbol{\sigma}dV \\ &= \int_A \left[\delta\boldsymbol{\varepsilon}^{\mathbf{0T}}\mathbf{N_b} + \delta\boldsymbol{\kappa}^{\mathbf{T}}\mathbf{M_b} + \delta\boldsymbol{\gamma}^{\mathbf{T}}\mathbf{Q}\right]dA \\ &= \boldsymbol{\delta}\mathbf{d}^{\mathbf{T}}\left[\mathbf{K} - \mathbf{K}_{\boldsymbol{\Delta T}} + \frac{1}{2}\mathbf{N1} + \frac{1}{3}\mathbf{N2}\right]\mathbf{d} - \boldsymbol{\delta}\mathbf{d}^{\mathbf{T}}\mathbf{P}_{\boldsymbol{\Delta T}}\end{aligned} \tag{13}$$

$$\begin{aligned}\delta W_{\text{ext}} = \int_A [&-I_0\left(\ddot{u}_0\delta u_0 + \ddot{v}_0\delta v_0 + \ddot{w}_0\delta w_0\right) \\ &- I_1\left(\ddot{u}_0\delta\phi_x + \ddot{\phi}_x\delta u_0 + \ddot{v}_0\delta\phi_y + \ddot{\phi}_y\delta v_0\right) \\ &- I_2(\ddot{\phi}_x\delta\phi_x + \ddot{\phi}_y\delta\phi_y) + p_a\delta w]dA \\ = &-\boldsymbol{\delta}\mathbf{d}^{\mathbf{T}}\mathbf{M}\ddot{\mathbf{d}} + \boldsymbol{\delta}\mathbf{d}^{\mathbf{T}}\mathbf{f}\end{aligned} \tag{14}$$

where, $\mathbf{d} = [\mathbf{u, v, w, \varphi_x, \varphi_y}]^T$ is the displacement vector and $(I_0, I_1, I_2) = \int_{-h/2}^{h/2}\rho(z)\cdot(1, z, z^2)dz$. In addition , $\mathbf{P}_{\boldsymbol{\Delta T}}, \mathbf{K}$, $\mathbf{K}_{\boldsymbol{\Delta T}}, \mathbf{N1}, \mathbf{N2}, p_a, \mathbf{M}$ and $\mathbf{f}$ are the thermal load vector, the linear elastic stiffness, the thermal geometric stiffness, the first-order nonlinear stiffness, the second-order nonlinear stiffness matrices, the aerodynamic pressure the mass matrix and the external force induced by thermal load, respectively.

Using the quasi-steady first-order piston theory (Ashley and Zartarian),

$$p_a(x,y,t) = -\frac{\rho_a V_\infty^{\ 2}}{\sqrt{M_\infty^{\ 2}-1}}\left\{\frac{\partial w}{\partial x} + \left(\frac{M_\infty^{\ 2}-2}{M_\infty^{\ 2}-1}\right)\frac{1}{V_\infty}\frac{\partial w}{\partial t}\right\} = -\left(\lambda\frac{D}{a^3}\frac{\partial w}{\partial x} + \frac{g_a}{\omega_0}\frac{D}{a^4}\frac{\partial w}{\partial t}\right) \tag{15}$$

where

$$\lambda = \frac{\rho_a V_\infty a^3}{\beta D},\quad D = \frac{E_m h^3}{12(1-\nu^2)},\quad g_{\text{a}} = \frac{\rho_a V_\infty(\beta^2-1)}{\beta^3\rho h\omega_0},\quad \beta = \sqrt{M_\infty^2-1},\quad \omega_0 = \left(\frac{D}{\rho_a h a^4}\right)^{\frac{1}{2}}$$

in here $\rho_a, V_\infty, M_\infty, \beta, D, \omega_0, g_{\text{a}}, \lambda$ and a represent the air mass density, the velocity of airflow, the Mach number, the aerodynamic pressure parameter, the flexural stiffness matrix, the convenient reference frequency, the non-dimensional aerodynamic damping, non-dimensional aerodynamic pressure and the panel length, respectively

Using Eq.(15), the last term of Eq.(14) can be written in the form as :

$$\begin{aligned}\boldsymbol{\delta}\mathbf{d}^{\mathbf{T}}\mathbf{f} &= \int_A p_a \delta w \, dA \\ &= -\int_A \left(\lambda \frac{D}{a^3}\frac{\partial w}{\partial x} + \frac{g_a}{\omega_0}\frac{D}{a^4}\frac{\partial w}{\partial t} \right) \delta w \, dA = -\boldsymbol{\delta}\mathbf{d}^{\mathbf{T}} \left(\lambda \mathbf{A}_{\mathbf{f}}\mathbf{d} + \frac{g_a}{\omega_0}\mathbf{A}_{\mathbf{d}}\dot{d} \right)\end{aligned} \tag{16}$$

where, $\mathbf{A_f}$, $\mathbf{A_d}$ denote the aerodynamic pressure matrix and the aerodynamic damping matrix, respectively.

Finally, the discretized form of governing equations obtained as:

$$\mathbf{M}\ddot{\mathbf{d}} + \frac{g_a}{\omega_0}\mathbf{A}_{\mathbf{d}}\dot{\mathbf{d}} + \left(\mathbf{K} - \mathbf{K}_{\Delta\mathbf{T}} + \lambda \mathbf{A}_{\mathbf{f}} + \frac{1}{2}\mathbf{N1} + \frac{1}{3}\mathbf{N2} \right)\mathbf{d} = \mathbf{P}_{\Delta\mathbf{T}} \tag{17}$$

The solution of Eq. (17) is assumed as $\mathbf{d} = \mathbf{d_s} + \Delta\mathbf{d_t}$, where $\mathbf{d_s}$ and $\mathbf{d_t}$ represent the time independent and time dependent solutions, respectively. Substituting the assumed solution into Eq.(17), we can obtain two sets of coupled governing equations as follows.

$$\left(\mathbf{K} - \mathbf{K}_{\Delta\mathbf{T}} + \lambda \mathbf{A}_{\mathbf{f}} + \frac{1}{2}\mathbf{N1}_{\mathbf{s}} + \frac{1}{3}\mathbf{N2}_{\mathbf{s}} \right)\mathbf{d}_{\mathbf{s}} = \mathbf{P}_{\Delta\mathbf{T}} \tag{18.a}$$

$$\mathbf{M}\ddot{\mathbf{d}}_{\mathbf{t}} + \frac{g_a}{\omega_0}\mathbf{A}_{\mathbf{d}}\dot{\mathbf{d}}_{\mathbf{t}} + \left(\mathbf{K} - \mathbf{K}_{\Delta\mathbf{T}} + \lambda \mathbf{A}_{\mathbf{f}} + \frac{1}{2}\mathbf{N1}_{\mathbf{s}} + \frac{1}{3}\mathbf{N2}_{\mathbf{s}} + \mathbf{N2}_{\mathbf{st}} + \frac{1}{2}\mathbf{N1}_{\mathbf{t}} + \frac{1}{3}\mathbf{N2}_{\mathbf{t}} \right)\mathbf{d}_{\mathbf{t}} = \mathbf{0} \tag{18.b}$$

where, the subscript s and t represent the static and dynamic state, respectively.

The Eq.(18.a) is used for the static problem, post-buckling analysis, and the Eq.(18.b) is for the dynamic problem such as flutter boundary and flutter. A small incremental time dependent solution, $\Delta\mathbf{d_t}$, is assumed and to linearize Eq.(18.b) the time dependent nonlinear stiffness matrices, $\mathbf{N1_t}$, $\mathbf{N}2_{\mathbf{t}}$ and $\mathbf{N2_{st}}$, become zero. Then the incremental equilibrium equation is expressed as:

$$\mathbf{M}\Delta\ddot{\mathbf{d}}_{\mathbf{t}} + \frac{g_a}{\omega_0}\mathbf{A}_{\mathbf{d}}\Delta\dot{\mathbf{d}}_{\mathbf{t}} + \left(\mathbf{K} - \mathbf{K}_{\Delta\mathbf{T}} + \lambda \mathbf{A}_{\mathbf{f}} + \mathbf{N1}_{\mathbf{s}} + \mathbf{N2}_{\mathbf{s}} \right)\Delta\mathbf{d}_{\mathbf{t}} = \mathbf{0} \tag{19}$$

A small amplitude vibration is assumed as $\Delta\mathbf{d}_t = \boldsymbol{\varphi}_0 e^{\omega t}$ and degree of freedom is reduced by Guyan reduction. Then, the reduced homogeneous equations for eigen analysis with state variables are written as

$$\left[\begin{bmatrix} \mathbf{0} & \mathbf{M_R} \\ \mathbf{K}_{\mathrm{R}} & \mathbf{C_R} \end{bmatrix} - \boldsymbol{\omega} \begin{bmatrix} \mathbf{M_R} & \mathbf{0} \\ \mathbf{0} & -\mathbf{M_R} \end{bmatrix} \right] \begin{Bmatrix} \varphi_0 \\ \dot{\varphi}_0 \end{Bmatrix} = 0 \tag{20}$$

where, $\mathbf{M_R}, \mathbf{K_R}$ and $\mathbf{C_R}$ are reduced mass, stiffness, damping matrices, respectively.

As λ increases gradually from zero, two of these eigen-values will approach each other and coalesce to ω^*_{cr} at $\lambda = \lambda_{cr}$. After that they become complex conjugate pairs such that $\omega = \omega_r \pm \mathrm{i}\omega_\mathrm{i}$ for $\lambda > \lambda_{cr}$. From here, the panel flutter occurs. The non-dimensional frequency, ω^*, in the figure is defined as:

$$\omega^* = \omega a^2 \sqrt{\frac{\rho_m h}{D_m}} \tag{21}$$

3. Numerical results and discussions

Various kinds of materials are used as a mixture of FGMs such as SiC/Al (Felman and Aboudi), Al_2O_3 / Ni (Na and Kim) SUS304/Si_3N_4 (Chen, Park and Kim) and Aluminum Oxide/Ti-6Al-4V (Park and Kim). Among these, we select a mixture of material such as SUS304/Si_3N_4, and then will investigate the post-buckling characteristics of the panels in supersonic airflows. Also the model is made up of temperature dependent materials with a square shape. In the finite element modeling, a 6×6 mesh is used, and nine-node plate element is chosen. Additionally, a selectively reduced integration (SRI) technique (Zienkiewicz et al.) is employed to prevent the transverse shear locking phenomena for thin plate model using first-order shear deformation theory. For the nonlinear analysis, the Newton-Raphson iteration scheme is adopted to obtain approximate solutions.

After the code verifications, the post-buckling behaviors and flutter boundary of FG panel subjected to supersonic aerodynamic loads are to be presented for two types of temperature variation such as uniform and gradient changes. In addition, influence of aerodynamic load of FG panels buckled by uniform temperature changes is dealt. Further, main aim of this study is to trace the temperature effects on the thermal post-buckling behaviors and flutter boundary of the FG panel, the results for the temperature dependant and independent material

properties are deeply investigated for the all clamped and simply supported boundary conditions. Especially, snap-through phenomena of simply supported case were thoroughly reported in the previous work for panel with temperature independent material(Sohn and Kim), thus only the quantitative difference resulting from the temperature dependent and independent properties are discussed briefly.

3.1. Code verifications

For the validation of the numerical results for the panel, three cases are chosen to compare with the previous data. First, the static stability boundary of clamped isotropic plate is compared with results of Xue and Mei. Table. 2 shows that the agreements between present results and previous data are satisfactory. Therefore, the application of the thermal and aerodynamic loads on a panel is validated in the iteration procedure using the Newton-Raphson method. Secondly, the thermal post-buckling behaviors of simply supported FG panel for $k=1$ are compared with previous data as shown in Fig.2. In the diagram, “A” denotes the curves for temperature dependent material properties. While, the group “B” represents the results for temperature independent material properties calculated just only at reference temperature, 300K. In here, the results of the groups “A” and “B” show good agreements for each case. Next, the critical pressures of simply supported FG panels for various volume fractions are compared with references (Sohn and Kim, Prakash and Ganapathi.). The results are shown in Table. 3 and agree well with that of previous work.

3.2. Thermal post-buckling of FG panels in supersonic airflows

The thermal post-buckling behaviors of FG panels in supersonic airflows are investigated with various volume fractions. In addition, the reference temperature and the thickness ratio(a/h) of the panel are taken 300K and 100, repectively. Prior to the discussions on the thermal post-buckling behaviors in supersonic airflows of the panel, Fig.3 shows the thermal

effect on the non-dimensionalized deflections of the clamped panel. Comparison of the data reveals that the deflections of the temperature dependent material case are larger than that of the temperature independent material as shown in the Figure. The reason may be originated from that internal thermal load leads the bifurcation of the model to appear at lower temperature than temperature independent material. The magnitude of the difference is increased in the sequences of metal, FGMs and ceramic. Fig.4 shows the comparative results of clamped panels with uniform temperature rise for $k=1$ and a/h= 60,80 and 100. As the model becomes thinner, the critical temperature is decreased. Also the differences are increased along with the increase of temperature. The gaps between temperature dependent and temperature independent case's are increased as the thickness ratios (a/h) are decreased because the thermal loads induce more in-plane load for thick plate.

Discussions of the numerical results for thermal post-buckling of the panels in a supersonic airflow are as follows. In Figs 5-8 and Figs 9-10 deals with the uniform and gradient temperature rise cases, respectively. Fig.5 (a) and (b) show the post-buckling behavior of panels for $\lambda = 0 \text{and } 200$, respectively. The panels have all clamped edges, and uniform temperature is elevated. As shown in Fig. 5(a), small amount of deviation is observed with respect to the temperature independent material model. But we have to remember that these results are very special case for the current sample calculation. Fig.5(b) reveals that the aerodynamics effect delays the appearance of the bifurcation on the panels. Also the deflection of the panel is decreased due to the aerodynamic pressure.

Fig. 6(a) and 6(b) depict the results for simply supported ceramic, FGM and ceramic panels for $\lambda = 0 \text{ and } 200$. Fig.6(a) shows small deviation between temperature dependent and independent case for curves A, B and C. The snap-through is appeared for curve "A" in this study, unlike the previous work considering the material properties as temperature independent. As shown in Fig.6(b), the snap-through is delayed due to aerodynamic loads.

Fig.7(a) indicates that the volume fractions index of the panels is increased then the critical temperatures are decreased. Since the panel is closer to metal which is less stiff than ceramic. In Fig.7(b), the volume fractions index is increased, the snap-through phenomena occur at lower temperature. In Fig.7(a) and Fig.7(b), when the aerodynamic loads are added, the appearance of bifurcation and snap-through phenomena are delayed

Fig.8 (a) and (b) show center deflection of the panel for $k=1$, which is buckled by a uniform temperature change with various temperature environments including simultaneous aerodynamic pressure. The temperature range is chosen based on the structural flutter boundary of the panel subjected to aero-thermal loads (Sohn and Kim). Fig.8 (a) presents the shape of the panel with all clamped boundary conditions at $\Delta T = 35, 40 \text{ and } 45\text{K}$, respectively. In here, a deformed shape of the panel has a symmetry image of its deformed direction to the opposite. The two curves for each temperature case have similar imagine each other, even though there are some differences since temperature effects on material properties. Moreover, a deformed panel becomes flat when the non-dimensional aerodynamic pressure has exceeded a critical value. Fig.8 (b) summarized the center deflections of simply supported panel at $\Delta T = 10, 15, 20 \text{ and } 25\text{K}$, respectively. Especially, at $\Delta T = 15K$, the panel has possibility of buckling in both directions, but in the temperature independent case, it buckles only in the downward direction. Further, there is just one equilibrium position for high aerodynamic pressures and the deflection is decreased, but not flat as in Fig.8(a)

Fig.9 and 10 show the thermal post-buckling behaviors of the panels for gradient temperature distributions of simply supported and clamped boundary condition, respectively. The temperature of the bottom surface, T_m, is fixed and the top surface, T_c, is increased gradually by ΔT_c, from 300K to $300\text{K}+\Delta T_c$. In Fig.9(a), the critical temperature is higher than uniform temperature case, and the differences of two curves for present and reference are larger than uniform temperature case in Fig.5(a). Since the thermal loads are imposed

only on the upper surface in gradient temperature case. In Fig.9(b), the critical temperature is also delayed as aerodynamic loads are applied.

In Fig. 10(a), the panel is deformed only upward direction at low temperatures. The interesting one is that there is no equilibrium position at the downward direction in the Sohn and Kim for ceramic(SUS304). Since they just studied the material properties as temperature independent, in-plane loads are estimated as smaller than present work. Another particular characteristic is that the deflection of a simply supported panel has different magnitudes depending on its deformed direction. However, in case of the clamped panel in Fig.9, it deflected either upward or downward directions with the same magnitude of non-dimensional deflection.

When the aerodynamic loads are added, the panels are deformed only in the upward direction. Since the aerodynamic pressures are imposed on the upper surface, they just deformed upward direction in Fig. 10(b)

3.3. Flutter boundary of FG panels in supersonic airflows

The critical aerodynamic pressure point is shown in Fig.11. As non-dimensional aerodynamic pressure, λ , are monotonously increased from zero and then two eigen-values merges. Here, λ_{cr} is considered to be the value λ at which the first coalescence occurs.

Flutter boundaries of FG panels subject to thermal and aerodynamic loads with uniform temperature changes are shown in Fig. 12(a) and (b). There are four types of panel behavior: flat and stable, aero-thermally buckled but dynamically stable, flutter (limit cycle oscillation) and chaos. Generally, thermal stresses can lower the flutter boundary of panels. With increasing of the temperature of panels, the critical dynamic pressure decreases as shown.

Fig.12 (a) depicts flutter boundaries of all clamped square FG panels. In the figure, the panels are flat and stable statically and dynamically at the “stable” region. While increasing the temperature, the panels are buckled but dynamically stable. Furthermore, the dynamic

pressure increases, limit cycle oscillations and chaotic motions are also observed. Flutter boundaries of all simply supported square FG panels is shown in Fig.12 (b). It is similar characteristics to the clamped cases. However, the critical aerodynamic pressure for flutter is lower than clamped one.

The critical fluttering value of various FG panels subject to thermal and aerodynamic loads with gradient temperature change are listed in Table.4. This comparison of the data reveals that the critical aerodynamic pressure of the temperature dependent material case (Present, Prakash and Ganapathi) are lower than that of the temperature independent material case (Sohn and Kim) as shown. The reason may be originated from that internal thermal load leads the more thermally induced panels to flutter at lower temperature than temperature independent material.

4. Conclusions

Functionally Graded (FG) panels are investigated for the thermal post-buckling characteristics, flutter boundary and aerodynamic loads. First-order shear deformation theory (FSDT) of the plate is applied to model the panel, and the von-Karman strain-displacement relations are adopted to account for large deflection. Further, the first-order piston theory is used to model the supersonic aerodynamic load. Material properties are assumed as temperature-dependent, and this is one of the essential features of the material at high temperature environments. Main aim of this study is to estimate the effect of temperature dependent characteristics of thermal post-buckling and flutter boundary of the FG panel composed of SUS304/Si_3N_4, and the results are discussed. It is concluded that the critical aerodynamic pressure decrease, as the value of volume fraction index, k , increases and the critical flutter velocity of a homogenous ceramic panel is the maximum among those of all panels. Comparing with isotropic metal panel (Si_3N_4), FG panels have a merit for flutter

characteristics. For more understanding the characteristics deviation due to the temperature and aerodynamic effects on the FG panels for applications, more parameter studies are required such as various mixture of materials, high temperature conditions and so on.

5. Acknowledgement

"This work was supported by the second stage of the Brain Korea 21 Project in 2007."

6. References

Ashley,H., Zartarian,G., 1956. Piston Theory-A New Aerodynamic Tools for the Aeroelastician, Journal of Aeronautical Science 23(12), 1109-1118

Chun, S. C., 2005. Nonlinear vibration of a shear deformable functionally graded plate Composite Structures 68(3), 295-302

Felman, E., Aboudi, J., 1997. Buckling analysis of functionally graded plated subjected to uniaxial loading. Composite Structures 38(1-4), 29-36.

Haddadpour, H., Navazi, H.M., Shadmehri, F., 2007. Nonlinear oscillations of a fluttering functionally graded plate. Composite Structures 79(2), 242-250

Javaheri, R., Eslami, M. R., 2002. Thermal buckling of functionally graded plates. AIAA Journal, 40(1), 162-169.

Kim, Y. W., 2005. Temperature dependent vibration analysis of functionally graded rectangular plates. Journal of Sound and Vibration 284(3-5), 531-549

Miyamoto, Y., Kaysser, W.A., Rabin B.H., Kawasaki, A., Gord, R. G., 1999. Functionally graded materials : Designg, Processing and Applications, Kluwer academic publishers, Boston, 1-6.

Na, K.-S., Kim, J.-H., 2006a., Thermal postbuckling investigations of functionally graded plates using 3-D finite element method. Finite Elements in Analysis and Design 42, 749-756.

Na, K.-S., Kim, J.-H., 2006b. Three-dimensional thermomechanical buckling analysis for functionally graded composite plates. Composite Structures 73(4), 413-422.

Park, J.-S., Kim, J.-H., 2006. Thermal postbuckling and vibration analyses of functionally graded plates. Journal of Sound and Vibration 289, 77-93.

Prakash, T., Ganapathi, M.,2006. Supersonic flutter characteristics of functionally graded flat panels including thermal effects. Composite Structures 72(1), 10-18.

Praveen, C.N., Reddy, J.N., 1998. Nonlinear transient thermoelastic analysis of functionally graded ceramic metal plates. International Journal of Solids and Structures 35(33), 4457-4476.

Prakash, T., Ganapathi, M., 2006. Supersonic flutter characteristics of functionally graded flat panels including thermal effects. Composite Structures 72(1), 10-18

Reddy, J. N., 2004. Mechanics of laminated composite plates and shells; Theory and Analysis, CRC PRESS.

Shen, H. S., 2007. Thermal postbuckling behavior of shear deformable FGM plates with temperature-dependent properties. International Journal of Mechanical Sciences 49(4), 466-478

Sohn, K. J., Kim, J. H., 2007. Structural stability of functionally graded panels subjected to aero-thermal loads. Composite Structures. accepted for publication

Touloukian,Y.S., 1967. Thermophysical Properties of High Temperature Solid Materials, MacMillan, New York.

Wu, L., 2004. Thermal buckling of a simply supported moderately thick rectangular FGM plate. Composite Structures 64(2), 211-218

Xue, D. Y., Mei, C., 1993. Finite element nonlinear panel flutter with arbitrary temperatures in supersonic floe. AIAA Journal 31(1), 154-62

Yang, J., Shen, H. S., 2003. Free vibration and parametric resonance of shear deformable functionally graded cylindrical panels. Journal of Sound and Vibration 261(5, 10), 871-893

Zienkiewicz,O.C., Taylor,R.L., Too,J.M., 1971. Reduced integration technique in general analysis of plates and shells. International Journal of Numerical Methods in Engineering 3,275-290.

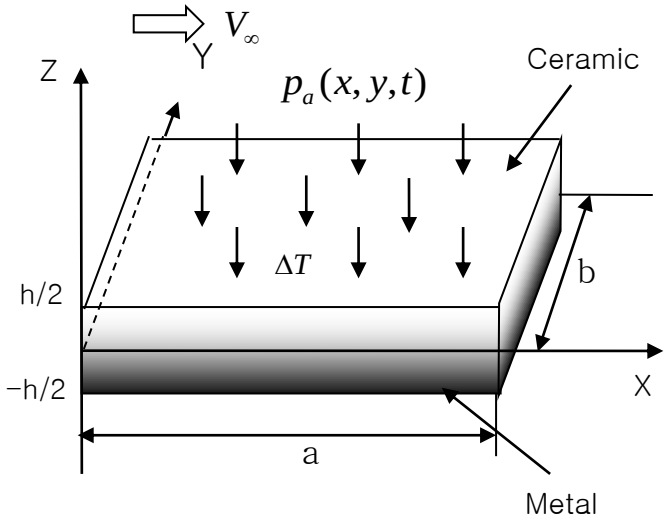

Fig.1 Geometry of a FG panel model under thermal load and supersonic airflows

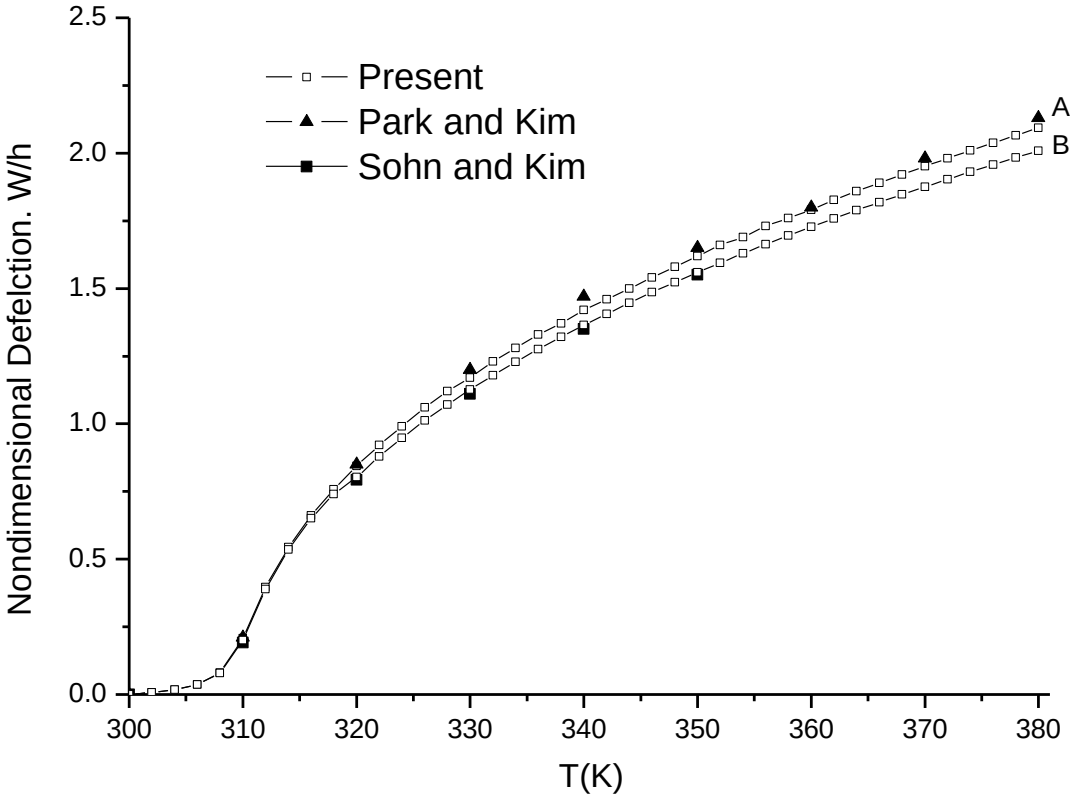

Fig.2 Thermal post-buckling behaviors of a square FG panel ($k = 1$)

(A : Temperature dependent, B : Temperature independent)

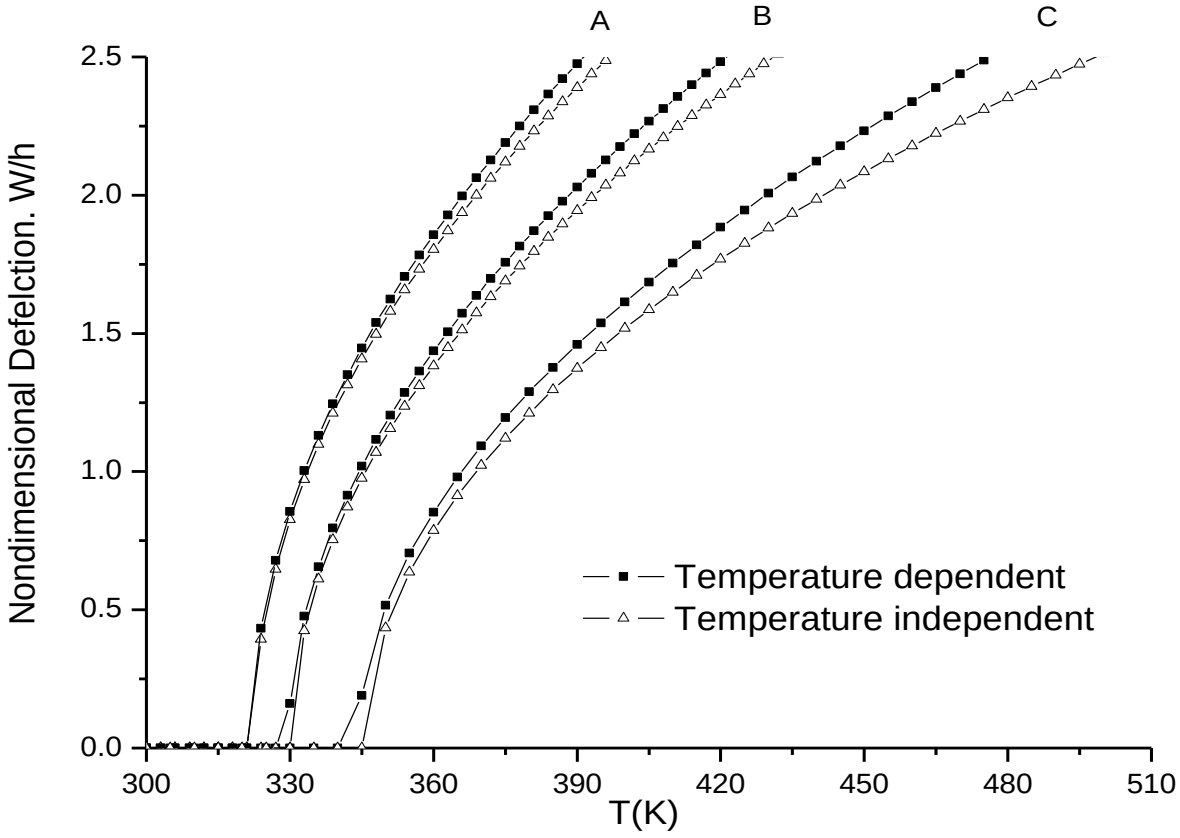

Fig.3 Temperature effect on the deflections of various square panel

(A : Metal(Si_3N_4), B : FGM($k=1$), C : Ceramic(SUS304))

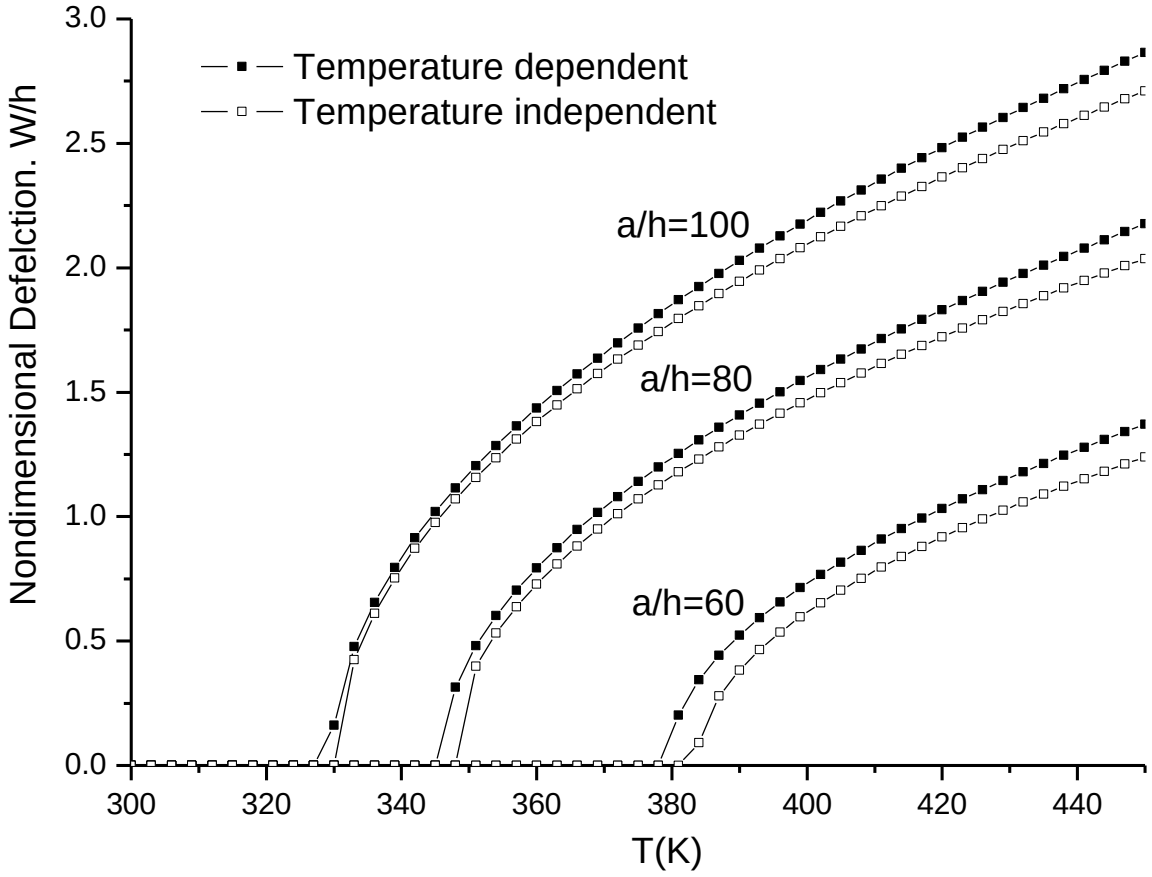

Fig.4 Thermal post-buckling characteristics of the FG panels under uniform temperature changes for various thickness ratio ($k=1$)

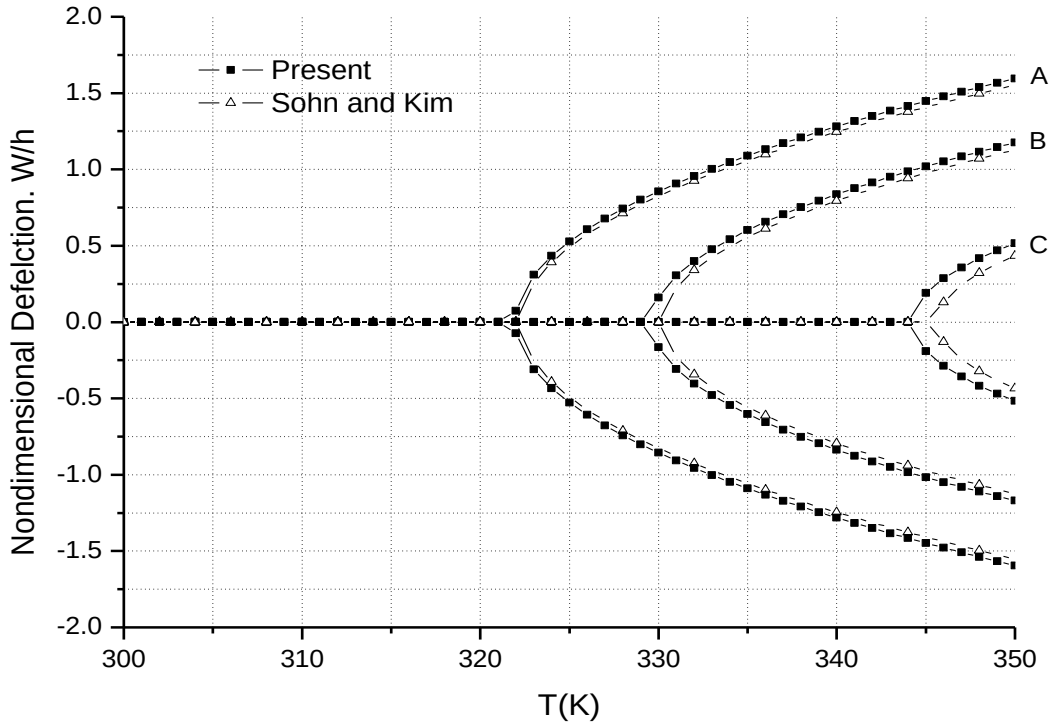

(a) Non-dimensional aerodynamic pressure, $\lambda = 0$

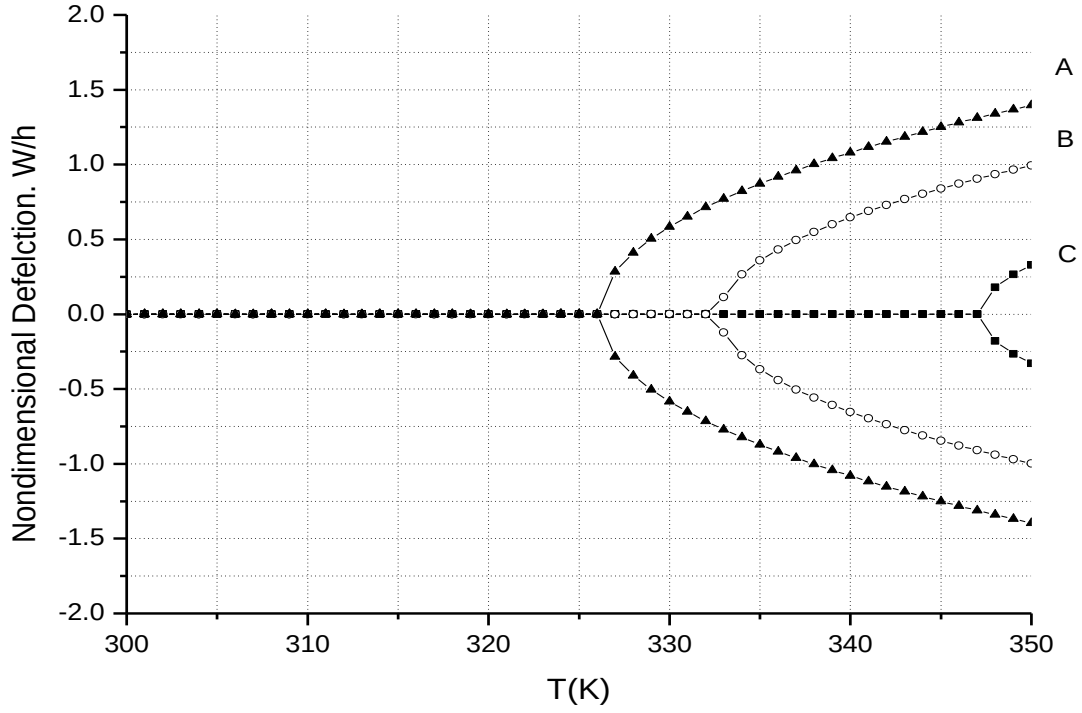

(b) Non-dimensional aerodynamic pressure, $\lambda = 200$

Fig.5 Thermal post-buckling characteristics of FG panels for uniform temperature changes

($T = 300\text{K} + \Delta T$ / A : Metal(Si_3N_4), B : FGM($k = 1$), C : Ceramic(SUS304))

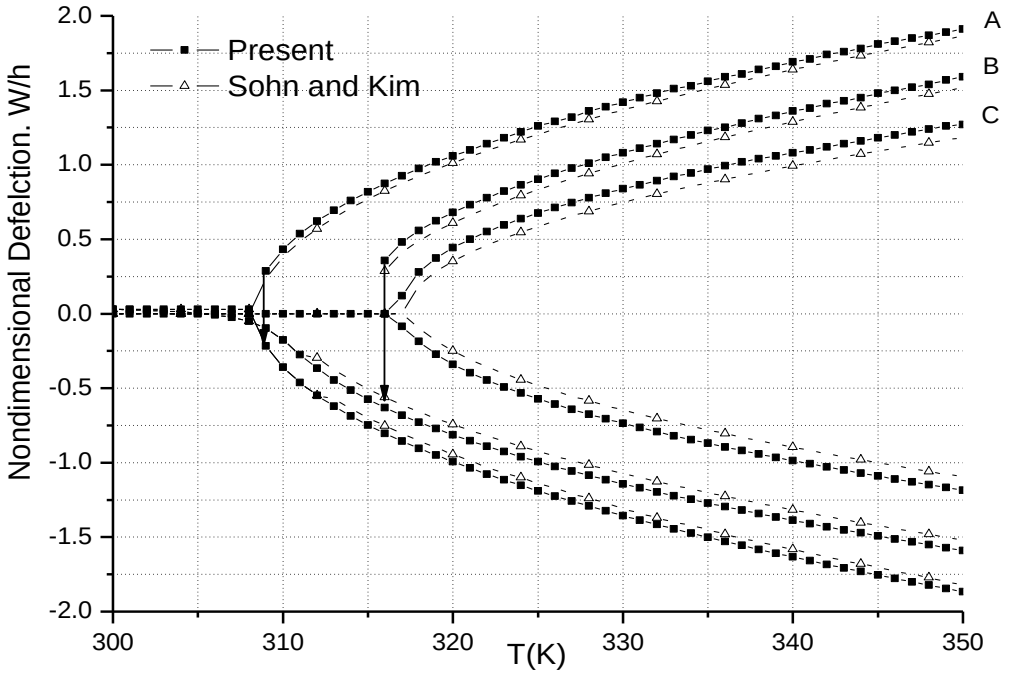

(a) Non-dimensional aerodynamic pressure, $\lambda = 0$

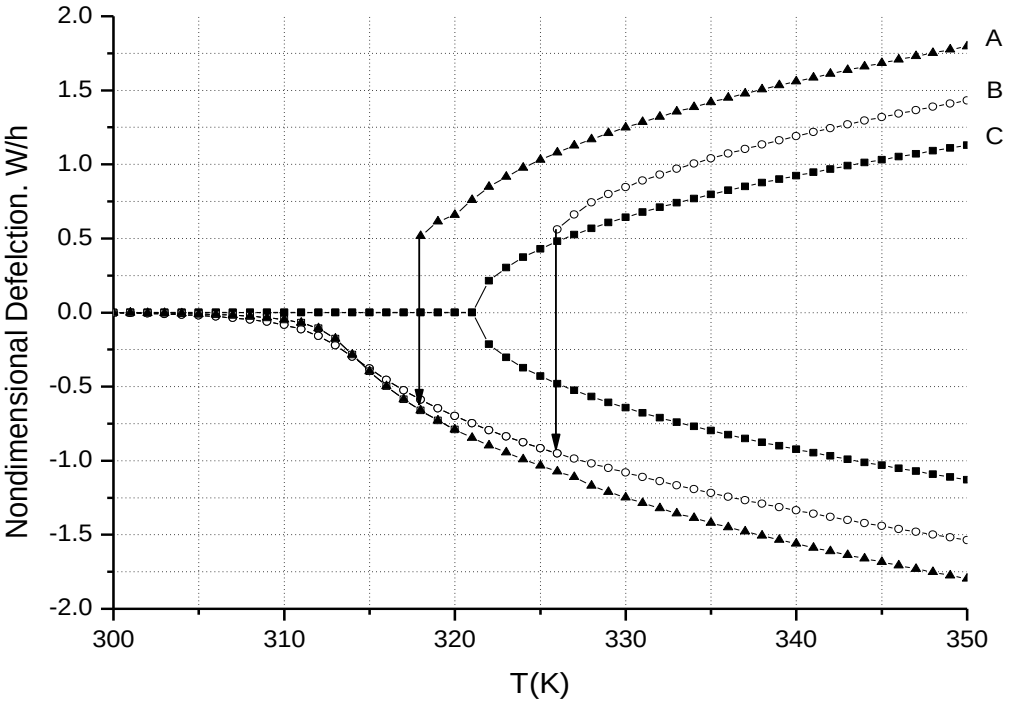

(b) Non-dimensional aerodynamic pressure, $\lambda = 200$

Fig.6 Thermal post-buckling characteristics of FG panels for uniform temperature changes

($T = 300\mathrm{K} + \Delta T$ /A : Metal(Si_3N_4), B : FGM($k = 1$), C : Ceramic(SUS304))

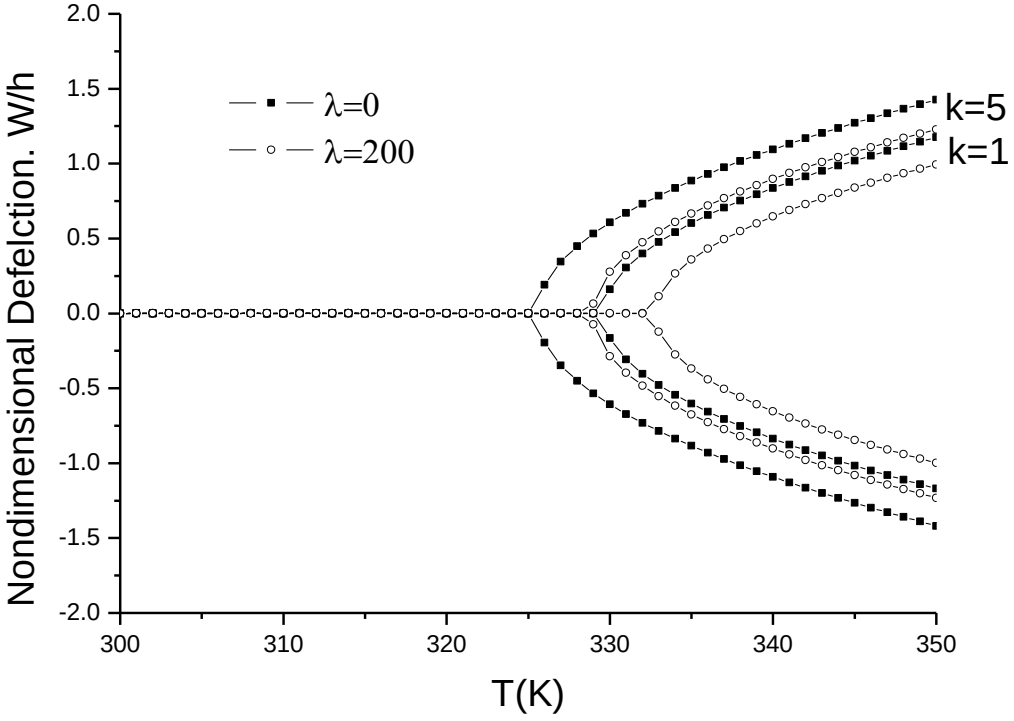

(a) Clamped boundary condition

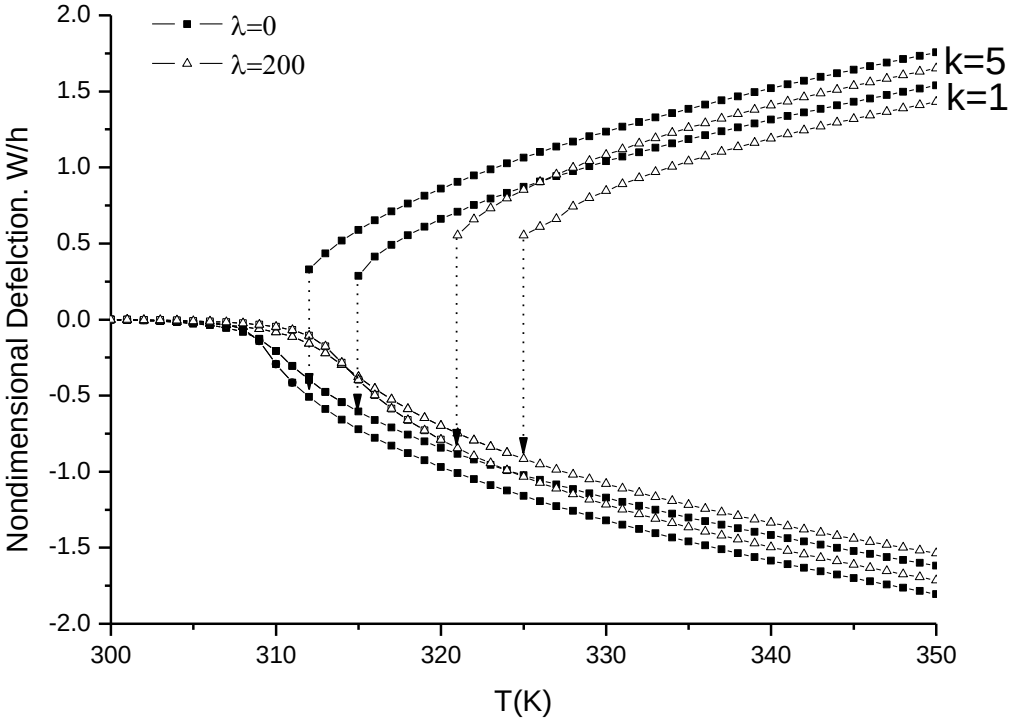

(b) Simply Supported boundary condition

Fig.7 Influences of non-dimensional aerodynamic pressure on FG panels under uniform temperature changes ($k = 1,5$)

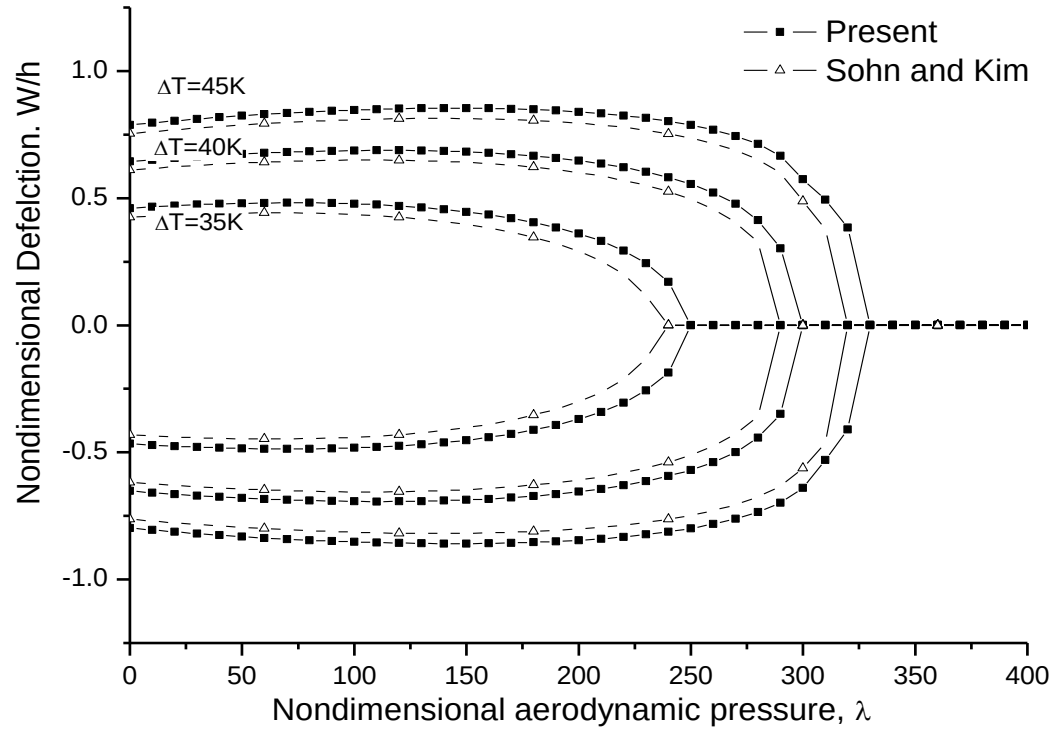

(a) Clamped boundary condition

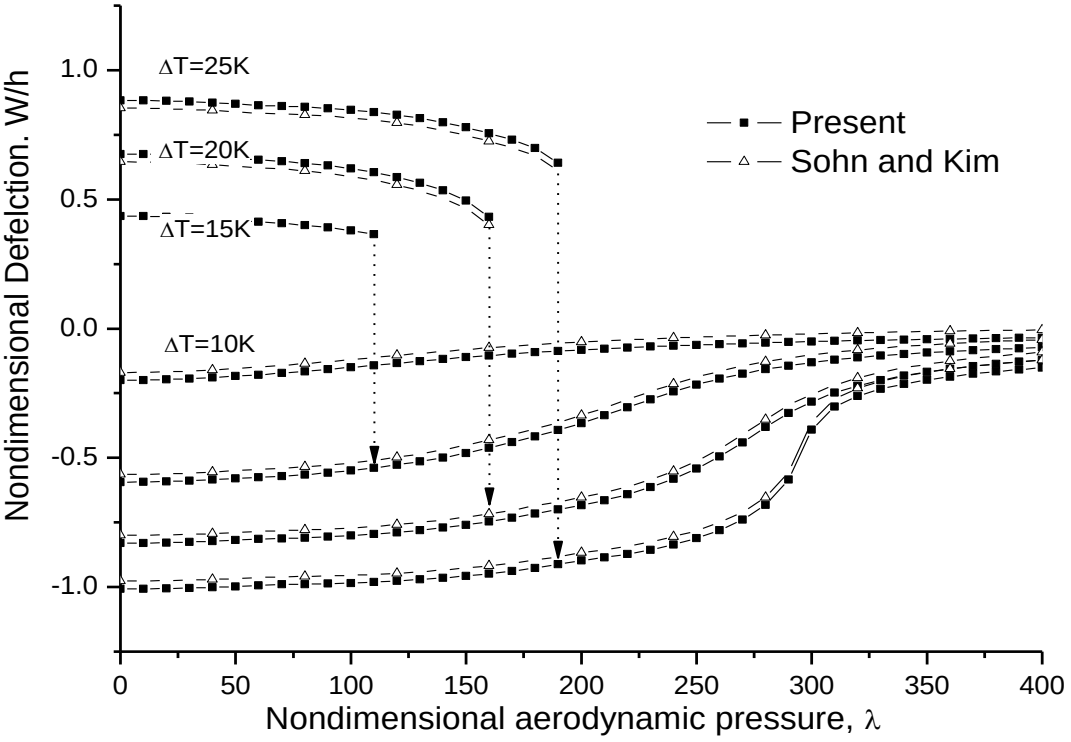

(b) Simply Supported boundary condition

Fig.8 Non-dimensional center deflections of an FG panel buckled by uniform temperature changes and aerodynamic pressures ($k=1$)

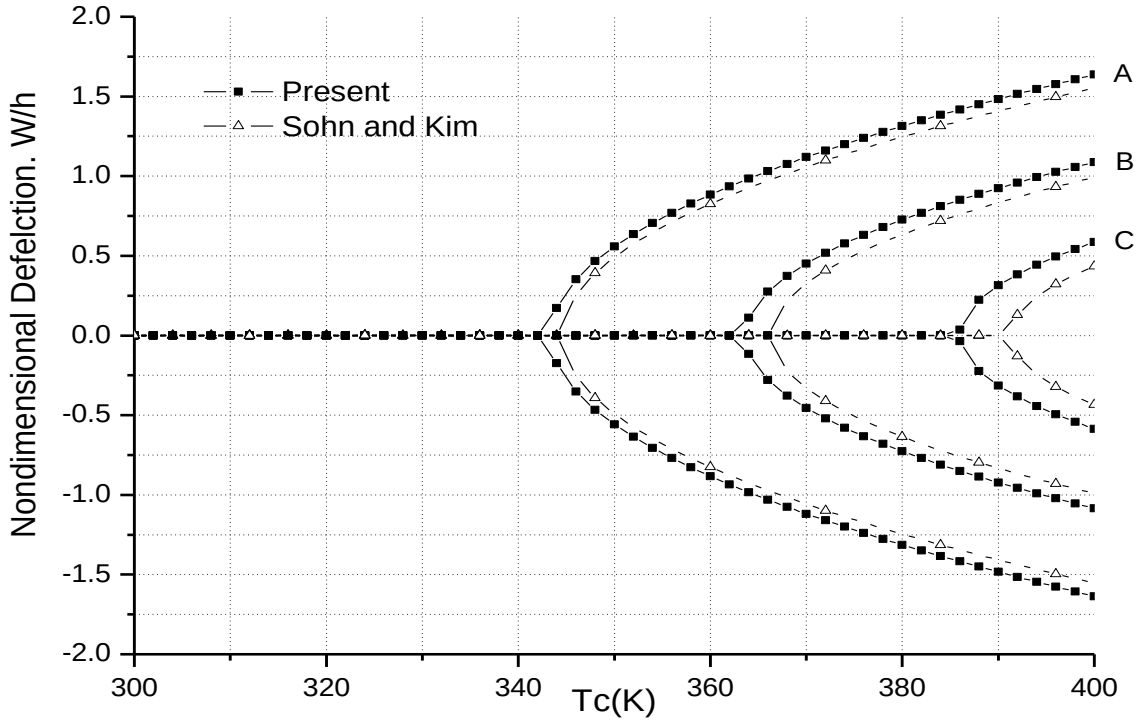

(a) Non-dimensional aerodynamic pressure, $\lambda = 0$

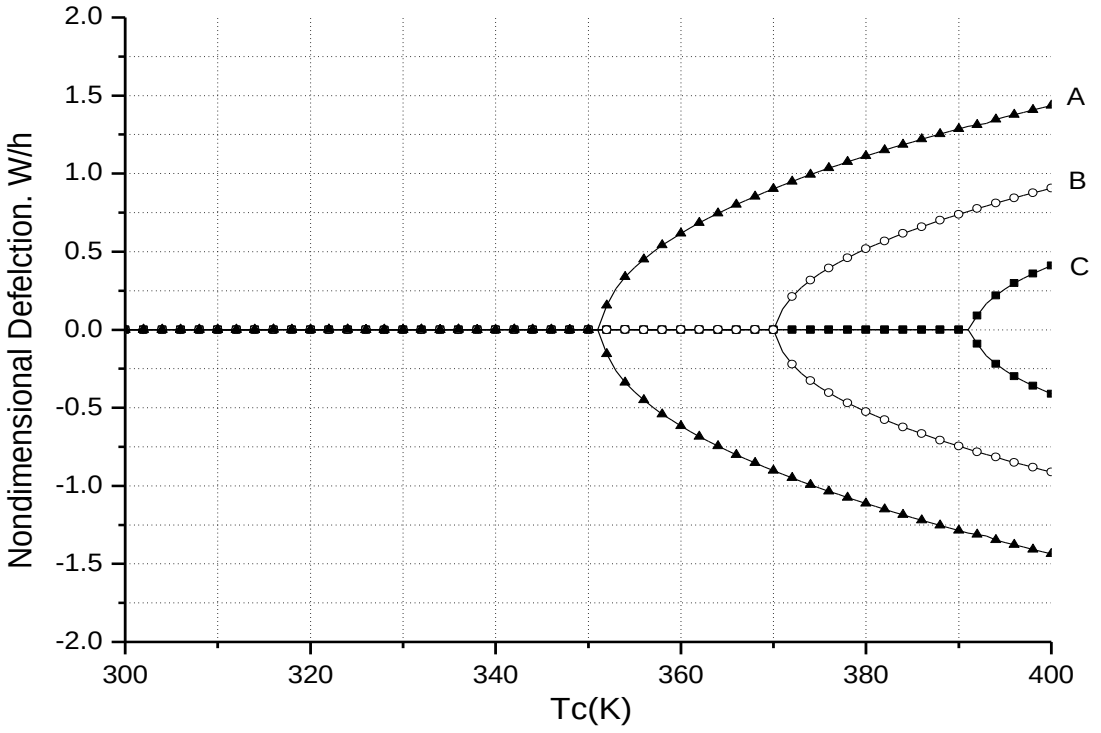

(b) Non-dimensional aerodynamic pressure, $\lambda = 200$

Fig.9 Thermal post-buckling characteristics of FG panels for gradient temperature changes
($T_m = 300\text{K},\ T_c = 300\text{K} + \Delta T_c$ / A : Metal(Si_3N_4), B : FGM($k = 1$), C : Ceramic(SUS304))

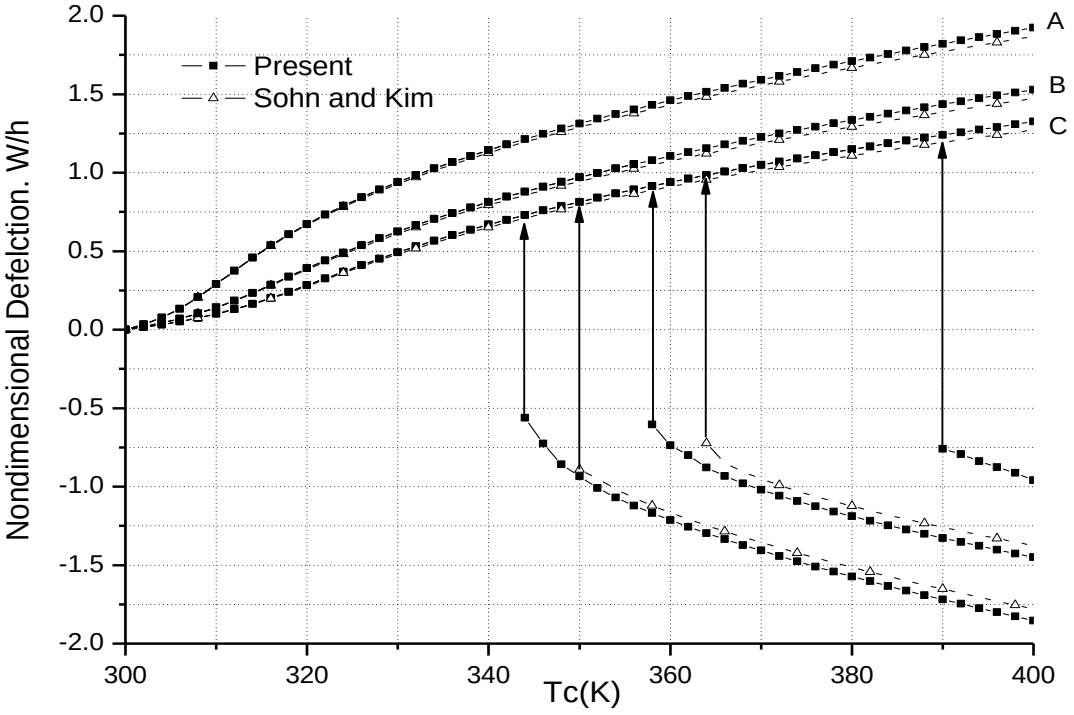

(a) Non-dimensional aerodynamic pressure, $\lambda = 0$

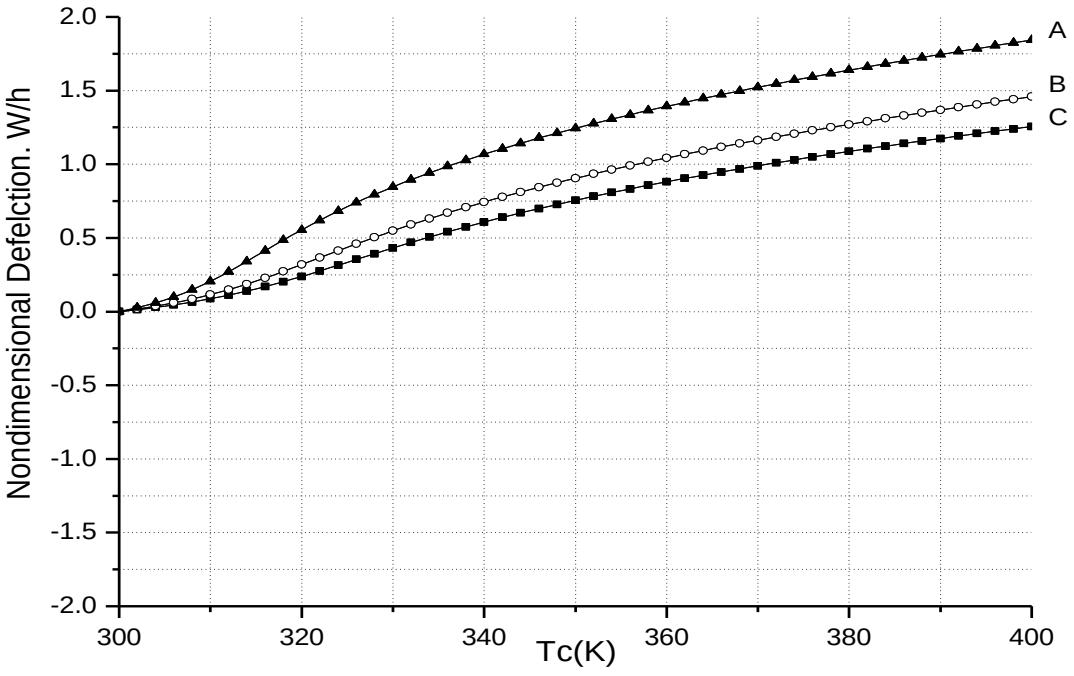

(b) Non-dimensional aerodynamic pressure, $\lambda = 200$

Fig.10 Thermal post-buckling characteristics of FG panels for gradient temperature changes
($T_m = 300\text{K},\ T_c = 300\text{K} + \Delta T_c$ / A : Metal(Si_3N_4), B : FGM($k = 1$), C : Ceramic(SUS304))

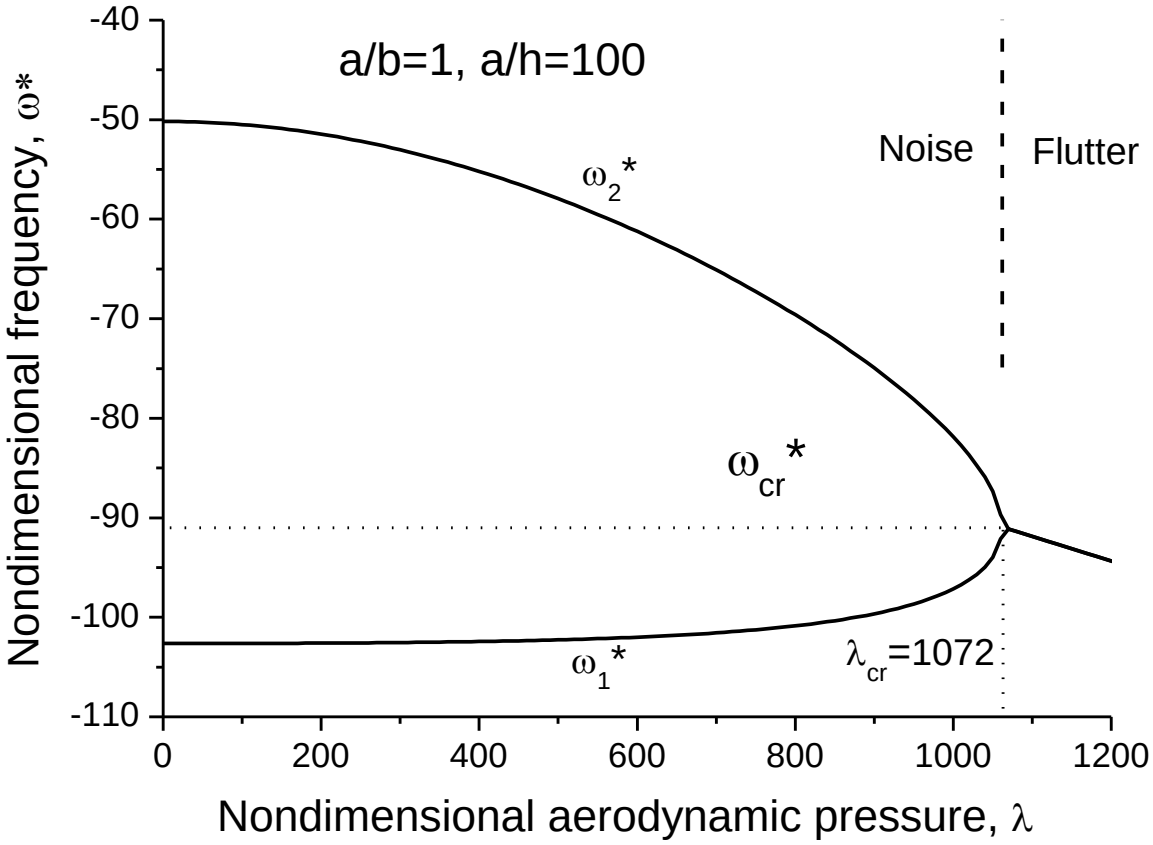

Fig. 11 Frequency coalescence for an FG panel ($\Delta T = 0$, $k = 1.0$)

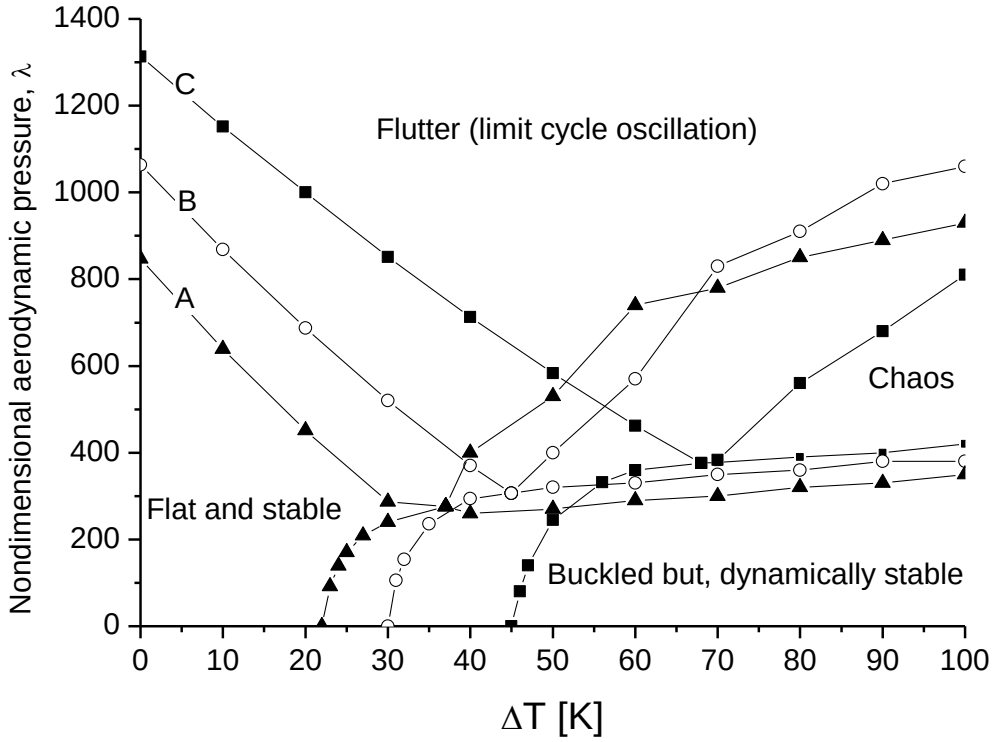

(a) Clamped boundary condition

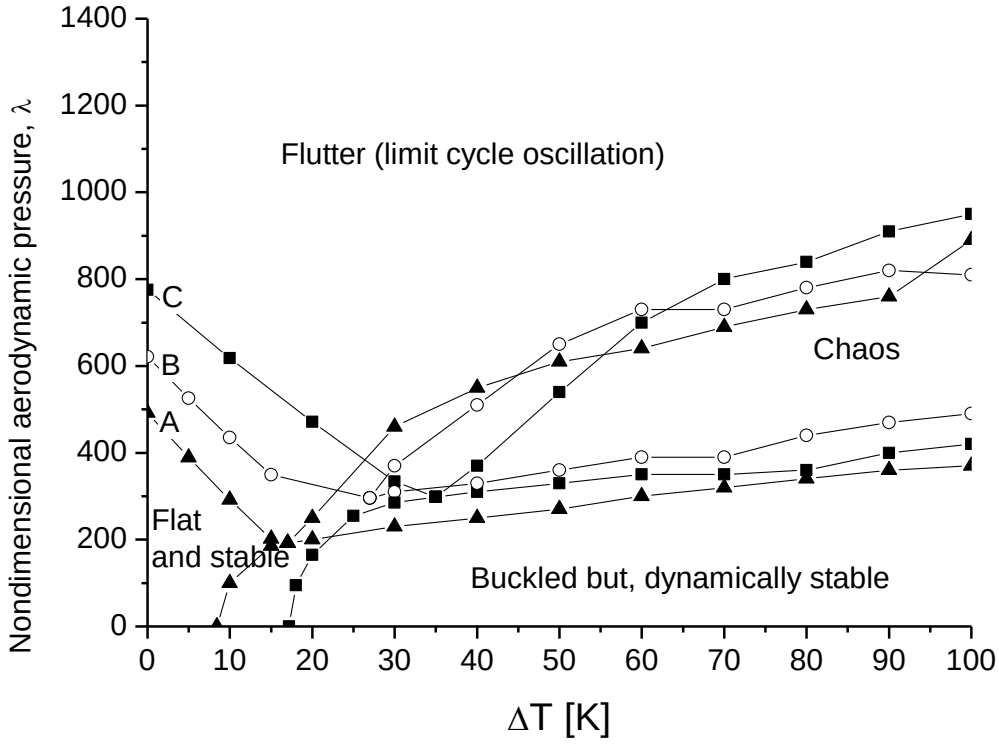

(b) Simply Supported boundary condition

Fig.12 Stability boundaries for various square panels for uniform temperature changes

($T = 300\mathrm{K} + \Delta T$ /A : Metal(Si_3N_4), B : FGM($k = 1$), C : Ceramic(SUS304))

Table 1. Material properties of FMGs for ceramic and metal (Yang and Shen)

	Materials	P_{-1}	P_0	P_1	P_2	P_3
E(Pa)	Si_3N_4	0	348.43×10^{9}	-3.070×10^{-4}	2.160×10^{-7}	-8.946×10^{-11}
	SUS304	0	201.04×10^{9}	3.070×10^{-4}	-6.534×10^{-7}	0
ρ (Kg/m^3)	Si_3N_4	0	2370	0	0	0
	SUS304	0	8166	0	0	0
α (1/K)	Si_3N_4	0	5.8723×10^{-6}	9.095×10^{-4}	0	0
	SUS304	0	12.330×10^{-6}	8.086×10^{-4}	0	0

Table 2. Static stability boundaries for a square isotropic plate (Xue and Mei)

		$\Delta T/\Delta T_{cr}$					
		1	1.2	1.4	1.6	1.8	2
Non-dimensional aerodynamic pressure	Xue and Mei. 1993	0	120	160	187	193	195
	Present	0	116	157	178	188	192

Table 3. Critical fluttering value of FG panels for gradient temperature change.

Volume fraction (k)	Sohn and Kim		Prakash and Ganapathi		Present	
	$\left\|\omega^*_{cr}{}^2\right\|$	λ_{cr}	$\left\|\omega^*_{cr}{}^2\right\|$	λ_{cr}	$\left\|\omega^*_{cr}{}^2\right\|$	λ_{cr}
0	9660.1	771.8	9661.35	775.78	9663.2	776.1
0.5	4573.6	663.0	4575.07	666.01	4575.3	669.1
1	3513.2	623.1	3515.57	625.78	3515.6	624.2
2.5	2698.2	588.0	2685.94	590.23	2689.8	592.3
5	2350.7	568.7	2348.72	571.48	2348.6	574.1

($T_m = T_c = 300K$, a/b=20, a/h=100)

Table 4. Critical fluttering value of FG panels for gradient temperature change.

Volume fraction (k)	Sohn and Kim		Prakash and Ganapathi		Present	
	$\left\|\omega^*_{cr}{}^2\right\|$	λ_{cr}	$\left\|\omega^*_{cr}{}^2\right\|$	λ_{cr}	$\left\|\omega^*_{cr}{}^2\right\|$	λ_{cr}
0	676.6	7950.8	647.65	7475.77	645.8	7470.8
0.5	561.9	3561.7	540.62	3381.36	542.3	3381.1
1	518.6	2683.5	499.61	2528.99	498.7	2523.5
2.5	477.6	1967.9	458.59	1849.33	455.2	1847.1
5	454.2	1684.9	433.20	1554.78	430.8	1552.4

($T_m = 300K$ and $T_c = 600K$, a/b=20, a/h=100)